Universal Extra Dimensions and Kaluza Klein Bound States

Christopher D. Carone,[*] Justin M. Conroy,[†] Marc Sher,[‡] and Ismail Turan[§]

Particle Theory Group, Department of Physics,

College of William and Mary, Williamsburg, VA 23187-8795

(Dated: December 2003)

Abstract

We study the bound states of the Kaluza-Klein (KK) excitations of quarks in certain models of Universal Extra Dimensions. Such bound states may be detected at future lepton colliders in the cross section for the pair production of KK-quarks near threshold. For typical values of model parameters, we find that "KK-quarkonia" have widths in the 10 - 100 MeV range, and production cross sections of order a few picobarns for the lightest resonances. Two body decays of the constituent KK-quarks lead to distinctive experimental signatures. We point out that such KK resonances may be discovered before any of the higher KK modes.

[*]carone@physics.wm.edu

[†]jconroy@camelot.physics.wm.edu

[‡]sher@physics.wm.edu

[§]ituran@newton.physics.metu.edu.tr

I. INTRODUCTION

The possibility of large extra dimensions has met considerable scrutiny in recent years. Sub-millimeter sized extra dimensions, in which only gravity can propagate in the bulk, allows for a reinterpretation of the hierarchy problem [1]. TeV-scale extra dimensions allow gauge and matter fields to propagate in the bulk as well, and have the virtue of allowing for an accelerated gauge unification [2]. These and related scenarios are well-motivated by string theory, where the existence of extra spatial dimensions is necessary for the consistency of the theory.

The notion that the propagation of gauge and matter fields in the bulk implies compactification radii of order a TeV^{-1} follows from consideration of precision electroweak constraints [3]. In the first types of models studied, at least one Higgs field was assumed to be confined to an orbifold fixed point. The vacuum expectation value (vev) of such a field necessarily results in mixing between the Z boson and its Kaluza-Klein (KK) excitations. One's intuition from models with extra Z' bosons and Z-Z' mixing suggests that the bounds on the first KK excitation will be of order a TeV, with some reduction if the vev of the Higgs responsible for this mixing is particularly small.

Universal extra dimensions (UED) were proposed as a way of avoiding such tree-level contributions to precision electroweak observables altogether [4]. In UED, all fields propagate in the bulk. Conservation of KK number prevents mixing between KK and zero-mode electroweak gauge bosons, so that the bounds described earlier are avoided. In the case of one extra dimension compactified on a Z_2 orbifold, a residual Z_2 symmetry of the effective four-dimensional (4D) Lagrangian allows interactions only between even numbers of the odd numbered KK modes. This renders the lightest KK particle (LKP) exactly stable. Typical bounds on the scale of compactification, $1/R$, are weakened to the collider bounds for the pair production of KK states, or approximately 300 GeV [5]. The possibility that the LKP is a dark matter candidate has also been investigated [6].

In the absence of radiative corrections and electroweak symmetry breaking, all KK modes at a given level would be exactly degenerate, with masses given by n/R, where n is a non-negative integer. Electroweak symmetry breaking introduces small corrections to this spectrum, with perhaps the exception of the KK excitations of the top quark, since m_{top} is not

necessarily much smaller than $1/R$. A more sizable effect results from loop corrections to the KK mass spectrum, which can be divided into two types [7]. There are finite corrections, resulting from the propagation of bulk fields around the compact dimension, which are insensitive to momentum scales above $1/R$. There are also logarithmically divergent contributions that are localized at the orbifold fixed points. These renormalize the possible 5D Lorentz-violating interactions that exist at the fixed points and alter the KK mass spectrum. If we think of these interactions as counterterms, a renormalization condition must be chosen to fix their finite parts. Corrections to KK masses are thus determined by $1/R$, the ultraviolet cutoff of the theory Λ, and the renormalization condition that determines the finite parts of the fixed-point-localized counterterms. Although in the most general case, these finite parts are undetermined (and the scenario is devoid of predictivity) one can adopt a minimal assumption that they vanish at the cutoff Λ. This boundary condition is no worse than, for example, the assumption of universal soft masses at the unification scale in the minimal supersymmetric standard model. We will adopt this assumption for the present purpose, and will show later that our results do not strictly depend on it.

A consequence of an otherwise degenerate mass spectrum corrected by loop effects is the possibility that some approximate degeneracies may remain. In particular, we note in the present work that the mass difference between the Kaluza-Klein excitations of the quarks (which we will refer to as KK-quarks, for brevity) and the LKP can be relatively small, for reasonable choices of R and Λ. The implication that we explore is the possible formation of KK-quark bound states, and we investigate whether they may be discerned at future electron-positron and muon colliders. In the case of heavy standard model quarks, it is well known that toponium bound states do not form because the lifetime of the top quark is short compared to the time scale associated with hadronization. It is usually said that this is a consequence of the heaviness of the top quark, but more precisely, it is a consequence of the large top-bottom mass difference. In the UED scenario of interest, the lightest KK quarks must decay to the (stable) LKP, and the phase space suppression leads to a different conclusion, for a wide range of model parameters. An investigation of KK bound states is not merely a topic of academic interest. It is possible that the pair production of KK modes of the first level may be accessible at colliders while that of the second level may be kinematically out of reach. Then the search for bound states of the first KK modes via a

threshold scan may be the quickest approach to discovering additional interesting physics.

Our paper is organized as follows. In the next section we give a detailed review of UED, including the topic of radiative corrections to the mass spectrum. In Section 3, we discuss the criterion for the formation of bound states, determine the model parameter space that is consistent with this constraint, and compute the bound state spectrum. In Section 4, we discuss the production and detection of "KK-quarkonia" at electron-positron, and at muon colliders. In particular, we show that the bound state decays have a distinctive signature that should allow easy discrimination from backgrounds. In the final section we summarize our conclusions.

II. UED

In this section we review the derivation of the 4D Lagrangian assuming one universal extra dimension. We begin by considering the simplified example of a U(1) gauge theory and then immediately generalize to the full standard model gauge group. We focus on results that will be used in the phenomenological analysis that follows.

Consider a 5D U(1) gauge theory with a fermion of unit charge e_{5D} propagating in the bulk. In 5D, the Clifford algebra is given by

$$\{\Gamma^M, \Gamma^N\} = 2g^{MN} \ , \tag{2.1}$$

where $\Gamma^\mu = \gamma^\mu$ and $\Gamma^5 = -i\gamma^5$. Here Roman indices run over all dimensions, while Greek indices run over the familiar four. It follows that the 5D spinor fields Ψ have four components, like their four-dimensional counterparts. However, since γ^5 no longer purely anticommutes with the 5D Dirac operator $i\Gamma^M \partial_M$, no chirality can be assigned to a massless 5D spinor field.

We now compactify the theory on the orbifold S^1/Z_2. Four-dimensional chirality is obtained by imposing the boundary conditions $\Psi(x^\mu, y) = \Psi(x^\mu, y + 2\pi R)$ and $\Psi(x^\mu, y) = -\gamma^5 \Psi(x^\mu, -y)$. This implies that there is a Z_2 even field Ψ_+ that is left-handed, and an odd field Ψ_- that is right handed,

$$\Psi_+(x^M) = \sum_{n=0}^{\infty} \Psi_+^{(n)}(x^\mu) \cos(ny/R) \ , \ \ \Psi_-(x^M) = \sum_{n=1}^{\infty} \Psi_-^{(n)}(x^\mu) \sin(ny/R) \ . \tag{2.2}$$

4

Since Ψ_- has no $n = 0$ component, only a left-handed zero-mode remains, while each higher KK level is composed of a vector-like pair. A 5D gauge field may be similarly decomposed

$$\mathcal{A}_\mu(x^M) = \sum_{n=0}^{\infty} \mathcal{A}_\mu^{(n)}(x^\nu) \cos(ny/R) \ , \ \ \mathcal{A}_5(x^M) = \sum_{n=1}^{\infty} \mathcal{A}_5^{(n)}(x^\nu) \sin(ny/R) \ . \tag{2.3}$$

This choice of Z_2 parities assures that an unwanted scalar photon zero mode is also projected away by the orbifold boundary conditions.

The 4D Lagrangian may be obtained by substituting these expansions into the 5D action

$$S = \int d^5x \left(\overline{\Psi} \, i\Gamma^M D_M \Psi - \frac{1}{4} F_{MN} F^{MN} + \mathcal{L}_{\text{gauge fixing}} \right) , \tag{2.4}$$

where $D^M = \partial^M - ie_{5D}\mathcal{A}^M$, and integrating over the extra dimension y. Terms quadratic in the nth mode $\Psi^{(n)}$ or $\mathcal{A}_\mu^{(n)}$ in the 4D theory are then found to be multiplied by a factor of $2\pi R$ if $n = 0$, or πR if $n = k > 0$. Thus, properly normalized kinetic terms are obtained only after the rescalings

$$\mathcal{A}_\mu^{(0)} = \frac{1}{\sqrt{2\pi R}} A_\mu^{(0)} \ , \quad \mathcal{A}_M^{(k)} = \frac{1}{\sqrt{\pi R}} A_M^{(k)} \ , \quad \Psi_+^{(0)} = \frac{1}{\sqrt{2\pi R}} \psi_+^{(0)} \ , \quad \Psi_\pm^{(k)} = \frac{1}{\sqrt{\pi R}} \psi_\pm^{(k)} \ . \tag{2.5}$$

Notice that the fields Ψ and $\mathcal{A}_\mu$ have mass dimensions 2 and 3/2, respectively, while the rescaled fields ψ and A_μ have their usual 4D mass dimensions. Taking these rescalings into account, and that derivatives with respect to y become factors of n/R in the 4D theory, one may easily find the tree-level masses

$$m_{\psi^{(n)}} = m_{A^{(n)}} = n/R \ . \tag{2.6}$$

The gauge field fermion interactions for the Z_2-even fermion fields follow from the 5D term

$$e_{5D} \, \overline{\Psi}_+ \mathcal{A}_\mu \gamma^\mu \Psi_+ \ . \tag{2.7}$$

Integrating over y, one finds

$$e_{5D} \left(2\pi R \overline{\Psi}_+^{(0)} \mathcal{A}^{(0)} \Psi_+^{(0)} + \sum_{n>0} \pi R \overline{\Psi}_+^{(0)} \mathcal{A}^{(n)} \Psi_+^{(n)} + \sum_{m>0,n,r} (\delta_{m,|n-r|} + \delta_{m,n+r}) \frac{\pi R}{2} \overline{\Psi}_+^{(m)} \mathcal{A}^{(n)} \Psi_+^{(r)} \right) . \tag{2.8}$$

Of relevance to our investigation of KK quark decays later are the gauge interactions involving $n = 0$ and $n = 1$ modes. With the field rescalings described above, and including the Z_2 odd fermion field one finds

$$\mathcal{L} = e \left(\overline{\psi}_+^{(0)} \slashed{A}^{(0)} \psi_+^{(0)} + \overline{\psi}_+^{(1)} \slashed{A}^{(0)} \psi_+^{(1)} + \overline{\psi}_-^{(1)} \slashed{A}^{(0)} \psi_-^{(1)} + [\overline{\psi}_+^{(0)} \slashed{A}^{(1)} \psi_+^{(1)} + h.c.] \right) , \tag{2.9}$$

where the 4D gauge coupling $e = e_{5D}/\sqrt{2\pi R}$. Note that the 5D gauge coupling e_{5D} has mass dimension $-1/2$, while e is dimensionless, as we expect. This expression may be written more compactly be embedding the left- and right-handed modes ψ_+ and ψ_- into Dirac spinors ψ

$$\mathcal{L}_{\text{LH}} = e \left(\overline{\psi}^{(0)} \slashed{A}^{(0)} P_L \psi^{(0)} + \overline{\psi}^{(1)} \slashed{A}^{(0)} \psi^{(1)} + [\overline{\psi}^{(0)} \slashed{A}^{(1)} P_L \psi^{(1)} + h.c.] \right) . \tag{2.10}$$

Here $P_L = (1 - \gamma^5)/2$, and the right-handed component of the zero-mode Dirac spinor is arbitrary. A similar expression for a fermion with a right-handed zero-mode can be obtained from Eq. (2.10) by replacing P_L by P_R. If radiative corrections render $m_{\psi^{(1)}} > m_{A^{(1)}} + m_{\psi^{(0)}}$ than the last term can lead to KK fermion decay.

The field rescalings and the KK mode numbers in Eq. (2.10) are all independent of the chosen gauge group. We therefore may immediately generalize to the standard model. The interaction terms relevant to the KK-quark decays that we consider later are as follows:

$$\begin{aligned}
\mathcal{L} &= \frac{2}{3}e \left[\frac{\sin(\theta_W + \theta_1) - \frac{1}{2}\sin(\theta_W - \theta_1)}{\sin 2\theta_W} \overline{u}^{(0)} \slashed{A}^{(1)} P_L u_L^{(1)} + \frac{\cos\theta_1}{\cos\theta_W} \overline{u}^{(0)} \slashed{A}^{(1)} P_R u_R^{(1)} \right] \\
&+ \frac{1}{3}e \left[\frac{\cos(\theta_W - \theta_1) + 2\cos(\theta_W + \theta_1)}{\sin 2\theta_W} \overline{u}^{(0)} \slashed{Z}^{(1)} P_L u_L^{(1)} - 2\frac{\sin\theta_1}{\cos\theta_W} \overline{u}^{(0)} \slashed{Z}^{(1)} P_R u_R^{(1)} \right] \\
&- \frac{1}{3}e \left[\frac{\sin(\theta_W + \theta_1) - 2\sin(\theta_W - \theta_1)}{\sin 2\theta_W} \overline{d}^{(0)} \slashed{A}^{(1)} P_L d_L^{(1)} + \frac{\cos\theta_1}{\cos\theta_W} \overline{d}^{(0)} \slashed{A}^{(1)} P_R d_R^{(1)} \right] \\
&- \frac{1}{3}e \left[\frac{2\cos(\theta_W - \theta_1) + \cos(\theta_W + \theta_1)}{\sin 2\theta_W} \overline{d}^{(0)} \slashed{Z}^{(1)} P_L d_L^{(1)} - \frac{\sin\theta_1}{\cos\theta_W} \overline{d}^{(0)} \slashed{Z}^{(1)} P_R d_R^{(1)} \right] \\
&+ \frac{1}{\sqrt{2}}e \left[\frac{1}{\sin\theta_W} \overline{u}^{(0)} \slashed{W}^{(1)} P_L d_L^{(1)} \right] + h.c.
\end{aligned} \tag{2.11}$$

Note that the $n = 1$ fields above are complete Dirac spinors (with both left- and right-handed components), and the subscript indicates only the chirality of the associated zero mode. In addition, θ_W is the zero-mode weak mixing (Weinberg) angle, while θ_1 is the corresponding angle for the $n = 1$ modes. In the absence of radiative corrections, the electroweak symmetry conserving contributions to the $B^{(1)}$-$W^{(1)}$ mass squared matrix are precisely diagonal (and equal to $1/R^2$), so that we expect $\theta_W = \theta_1$. In that limit, the photon and Z couplings in Eq. (2.11) have the same values as their couplings to either left- or right-handed up or down quarks. However, radiative corrections lead to much smaller values of θ_1. For example, for $\Lambda R = 20$ and $R^{-1} = 500$ GeV, $\sin^2\theta_1 \approx 10^{-2}$ [7]. In the following section, we omit the dependence on θ_1 to streamline our analytical expressions. The full dependence on θ_1 has

6

been taken into account in all our numerical results, and complete analytical expressions are provided in the Appendix.

Radiative corrections to the KK-gauge boson and KK-quark masses allow for two-body decays via the interactions in Eq. (2.11). Over the range of ΛR and R^{-1} that we consider, the LKP is the first KK excitation of the photon, $\gamma^{(1)}$ [7]. The radiative corrections to the KK-quark and the KK-gauge boson masses were calculated by Cheng, Matchev and Schmaltz [7]. Adopting their assumption that the finite parts of counter terms vanish at the cutoff scale Λ, we plot the mass splitting between the KK-quarks and the LKP, as well as the splitting between the weak KK-gauge bosons and the LKP, as a function of $1/R$, in Fig. 1, setting the value of $\Lambda R = 20$. Complete expressions for the radiative corrections that are taken into account in this figure can be found in Ref. [7]. As a consequence of the smallness of the $n = 1$ mixing angle θ_1, the LKP, $\gamma^{(1)}$, is almost entirely a KK-B boson, while the KK-W and KK-Z are virtually degenerate in mass. As we will see in the next section, the values of ΔM in Fig. 1 are small enough to lead to KK-quark bound state formation.
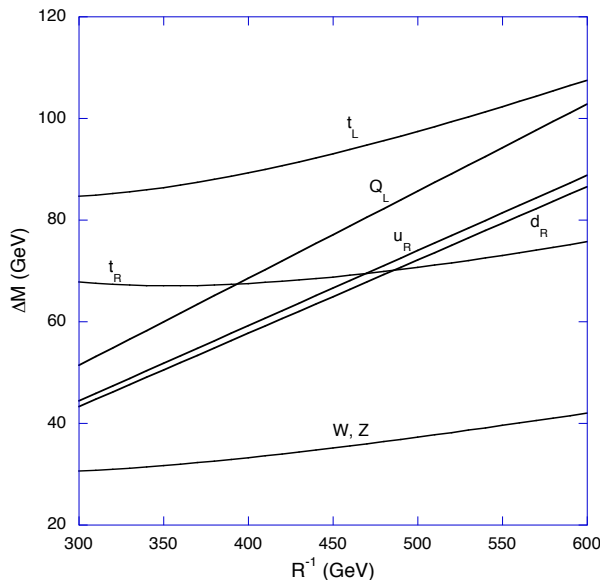

FIG. 1: The mass splitting between KK-quarks and the LKP, $\gamma^{(1)}$, as well as the splitting between the weak KK-gauge bosons and the LKP, as a function of $1/R$ for $\Lambda R = 20$. Here, Q_L stands for all isodoublet KK-quarks except top, u_R for up and charm isosinglet KK-quarks, and d_R for down, strange and bottom isosinglet KK-quarks

III. BOUND STATES

From Fig. 1, one finds that radiative corrections to the KK masses in UED are typically in the 10-100 GeV range. We will show that this is numerically small enough to allow for the formation of bound states of KK quarks. The smaller phase space available for KK-quark decay renders the bound states narrower than the spacing between adjacent KK-quarkonia levels, at least for the first few levels. In this section, the decay widths and branching ratios of the KK-quarks are calculated and discussed, as well as the mass splittings of the different KK-quarkonia energy levels and the production cross sections at lepton colliders.

A. Decay widths and branching ratios

With the Lagrangian and mass splittings given in the previous section, it is straightforward to determine the decay widths and branching ratios of the KK-quarks. We will begin by considering the weak isosinglet KK-quarks (except the KK-top), then the weak isodoublet KK-quarks, and finally the unusual case of the isosinglet KK-top quark. While the partial decay widths of KK-quarkonia through annihilation are typically tens of keV, we will see that the decay widths of the KK-quarks (except the KK-top) are typically close to a hundred MeV. Thus, the decay width of a KK-quarkonium state will be twice the decay width of the KK-quark.
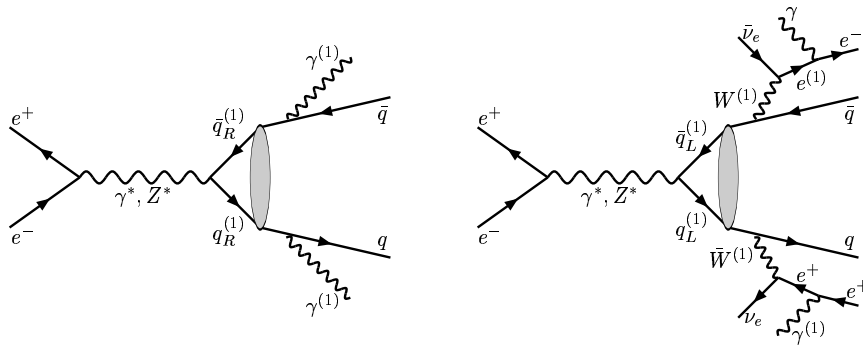

FIG. 2: The production and decay chains of $q_R^{(1)}$ and $q_L^{(1)}$ pairs. Note that all of the decays in the $q_L^{(1)}$ decay chain are two-body, leading to monochromatic quarks and leptons.

1. Isosinglet KK-quarks

Isosinglet KK-quarks cannot decay into KK-W bosons and their decay into KK-Z bosons is suppressed by a factor of $\sin^2\theta_1$. In addition, their decay into KK-Higgs bosons is suppressed by small Yukawa couplings. As a result, the dominant decay mode is $q^{(1)} \to q^{(0)}\gamma^{(1)}$, as shown in Fig. 2. Since the LKP is stable, the decay signature will be a monochromatic quark and missing energy. The one exception is the isosinglet KK-top quark, which cannot decay into a top quark and the LKP; we will discuss that case shortly. Including the small coupling to the KK-Z boson, we find that the branching ratio into a quark and a KK-γ is over 98 percent (consistent with the results in [8]). Neglecting the mass of the light quark and $\sin^2\theta_1$, we find the decay width

$$\Gamma(d_R^{(1)} \to d_R\,\gamma^{(1)}) = \frac{e^2 m_{d_R^{(1)}}}{288\pi \cos^2\theta_W} \left(1 - \frac{m_{\gamma^{(1)}}^2}{m_{d_R^{(1)}}^2}\right)^2 \left(2 + \frac{m_{d_R^{(1)}}^2}{m_{\gamma^{(1)}}^2}\right) . \tag{3.1}$$

An exact expression is given in the Appendix. The decay width for the $u_R^{(1)}$ is larger by a factor of four. Given values for $1/R$ and ΛR, this width is completely determined. The results are shown in Fig. 3. We see that the widths are typically within a factor of two of 10 MeV. As noted above, the decay signature is a monochromatic quark and missing energy; for $1/R = 500$ GeV and $\Lambda R = 20$, the quark energy is 67 GeV.

2. Isodoublet KK-quarks

For the isodoublet KK-quarks, decay channels into KK-W and KK-Z bosons are available. Although there is less phase space into these than into the KK-γ boson, the couplings are substantially larger, and the KK-W and KK-Z modes dominate. The decay width into a KK-W is given by

$$\Gamma(d_L^{(1)} \to u_L\,W^{(1)}) = \frac{e^2 m_{d_L^{(1)}}}{64\pi \sin^2\theta_W} |V_{ij}|^2 \left(1 - \frac{m_{W^{(1)}}^2}{m_{d_L^{(1)}}^2}\right)^2 \left(2 + \frac{m_{d_L^{(1)}}^2}{m_{W^{(1)}}^2}\right) , \tag{3.2}$$
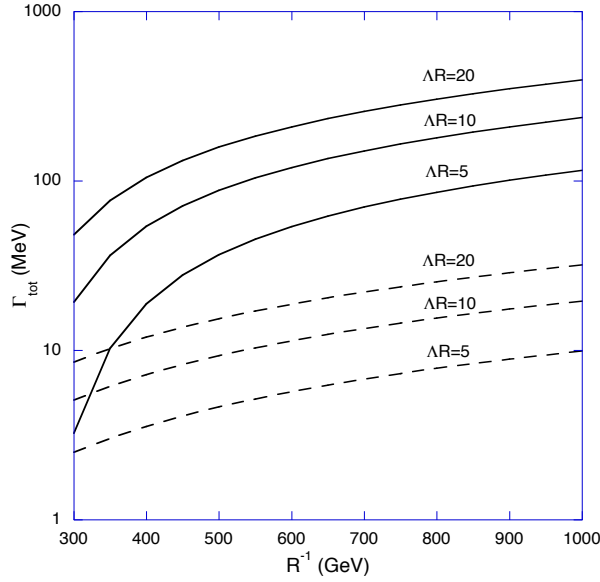
FIG. 3: The total decay width of $n = 1$ isosinglet and isodoublet down KK-quarks as a function of R^{-1} for fixed $\Lambda R = 5, 10, 20$. The solid lines represent the total decay widths of isodoublet down KK-quarks for each corresponding ΛR value, respectively. The dashed lines are for the isosinglet case. The isodoublet up KK-quark total decay width is equal to that of the down and the isosinglet up KK-quark's width is four times larger than that of the isosinglet down.

where V_{ij} is the relevant CKM element. The identical decay width, of course, applies to $u_L^{(1)} \to d_L W^{(1)}$ decays. The decay width into a KK-Z is given by

$$\Gamma(d_L^{(1)} \to d_L Z^{(1)}) = \frac{e^2 m_{d_L^{(1)}}}{128\pi \sin^2 \theta_W} \left(1 - \frac{m_{Z^{(1)}}^2}{m_{d_L^{(1)}}^2}\right)^2 \left(2 + \frac{m_{d_L^{(1)}}^2}{m_{Z^{(1)}}^2}\right) . \qquad (3.3)$$

We see that the branching ratio into the KK-W bosons are $2|V_{ij}|^2$ times that of the KK-Z bosons. The branching ratio into KK-γ bosons is negligible, always less than a few percent. These decays will give spectacular signatures. The decay into a KK-W boson, as shown in Fig. 2, leads to the decay chains $d_L^{(1)} \to u_L W^{(1)} \to u_L l \nu^{(1)}$ and $d_L^{(1)} \to u_L W^{(1)} \to u_L l^{(1)} \nu \to u_L l \nu \gamma^{(1)}$ leading to a monochromatic quark, a lepton, and missing energy. For example, for $1/R = 500$ GeV and $\Lambda R = 20$, the quark energy will be 46 GeV. Assuming measurement of the quark jet allows reconstruction of the $W^{(1)}$ four-momentum, then the lepton energy can

10

be completely determined[1]. The decay into a KK-Z is even more spectacular, with the chain $d_L^{(1)} \rightarrow d_L \, Z^{(1)} \rightarrow d_L \, l \, l^{(1)} \rightarrow d_L \, l \, l \, \gamma^{(1)}$, where l is a charged lepton. Again, the initial quark jet energy is fixed, and the sequential two-body decays should allow for easy reconstruction of the event, and suppression of backgrounds. Of course, in both the KK-W and KK-Z cases, there will also be hadronic decays – we have focused on the leptonic because the signatures are much cleaner. The resulting total widths are plotted in Fig. 3; and the KK-W final state accounts for 2/3 of the widths (for the first two generations).

For the first two generations, generation-conserving decays are favored, since the CKM matrix is nearly the identity. However, for the third generation, a decay into a top quark is not kinematically allowed. For the KK-top quark, this means that only the decay into a KK-W is possible. Due to CKM suppression, decays of the KK-bottom into KK-Z and KK-γ are favored and thus the decay width of the KK-bottom is 1/3 of those shown in Fig. 3. For the isodoublet KK-top, the mass is somewhat larger than the other KK-quarks, and thus more phase space is available. For most of parameter-space, we find that the decay width of the KK-top (entirely through the KK-W chain) is approximately 80 percent of the widths shown in the figure.

3. isosinglet KK-top quarks

The isosinglet KK-top quark has a very different decay signature. Flavor-conserving decays are kinematically forbidden, while flavor-changing decays are not possible since there is no coupling to the KK-W. Hence, there are no two-body decays at tree-level. The isosinglet KK-top can decay into a KK-γ and a virtual top quark, which then decays into a bottom quark and a virtual W, which then decays. This four-body decay will be strongly phase-space suppressed. One expects four-body phase space to be roughly 10^{-4} of two-body phase space, and this leads to a decay width of the isosinglet KK-top of approximately $1 - 10$ keV. This is small enough that the annihilation of the KK-quarkonia will dominate. As we will see in the next section, the annihilation width into electron pairs will be $10 - 20$ keV, and when the other annihilation channels (other leptons and quarks) are included, the

---

[1] Even if the $W^{(1)}$ four-momentum can't be reconstructed, the spread in the lepton energy will be $\mathcal{O}(10\%)$.

total width will be well over a hundred keV. Thus, the dominant decay mechanism will be primarily into fermion-antifermion pairs, and there will be no missing energy in the decay.

B.   Production cross-sections

The cross-section for production of a vector resonance, $e^+e^- \to V \to X$ is given by [9]

$$\sigma_V = \frac{12\pi(s/M_V^2)\Gamma_{ee}\Gamma_X}{(s - M_V^2)^2 + M_V^2\Gamma_V^2} , \tag{3.4}$$

where Γ_{ee}, Γ_X and Γ_V are the partial widths for $V \to e^+e^-$, for $V \to X$ and for the total width, respectively. Since we are interested in the total production cross-section, and since the partial width into Γ_{ee} is much smaller than the total width, we can set $\Gamma_X = \Gamma_V$ (this will be valid for all cases except the isosinglet KK-top quarkonia). At the peak resonance, the production cross-section is then given by

$$\sigma_V^{\text{peak}} = \frac{12\pi}{M_V^2}\frac{\Gamma_{ee}}{\Gamma_V} . \tag{3.5}$$

We need the partial decay width of $V \to e^+e^-$. The decay width through a virtual photon is given by

$$\Gamma(V \to \gamma^* \to e^+e^-) \equiv \Gamma_\gamma = \frac{4\pi\alpha e_Q^2}{3M_V^3}|F_V|^2\left[1 - \frac{16\alpha_s}{3\pi}\right] , \tag{3.6}$$

where $|F_V|^2$ is related to the wave function at the origin, and is given by $12M_V|\Psi_V(0)|^2$. The partial decay width including virtual Z exchange is related to this

$$\Gamma(V \to \gamma^*, Z^* \to e^+e^-) = (M_V^2/e^2e_Q)^2(|G_V|^2 + |G_A|^2)\Gamma_\gamma , \tag{3.7}$$

where

$$G_V = \frac{e^2e_Q}{M_V^2} + \frac{8G_FM_Z^2}{\sqrt{2}}\frac{g_V^e g_V^Q}{M_V^2 - M_Z^2 + i\Gamma_ZM_Z} , \tag{3.8}$$

and

$$G_A = \frac{8G_FM_Z^2}{\sqrt{2}}\frac{g_A^e g_V^Q}{M_V^2 - M_Z^2 + i\Gamma_ZM_Z} . \tag{3.9}$$

Here, g_V and g_A are the vector and axial vector couplings of the fermion to the Z, and $g_{V_L}^Q = g_{Q_L}$, $g_{V_R}^Q = (g_{Q_L} + g_{Q_R})/2$ with $g_Q = T_3 - e_Q\sin^2\theta_W$. Finally, we need the wave function at the origin. At these high mass scales, one expects single gluon exchange to be fairly accurate, and in that approximation the wave function at the origin is given by

$$|\Psi(0)|^2 = \frac{1}{\pi}\left(\frac{2M_Q\alpha_s(M_Q)}{3n}\right)^3 , \tag{3.10}$$

TABLE I: The partial decay width of $V \to e^+ e^-$ for both isodoublet and isosinglet KK-quark bound states .

M_V(GeV)	$\Gamma_{ee}(\bar{u}_L^{(1)} u_L^{(1)})$(keV)	$\Gamma_{ee}(\bar{d}_L^{(1)} d_L^{(1)})$(keV)	$\Gamma_{ee}(\bar{u}_R^{(1)} u_R^{(1)})$(keV)	$\Gamma_{ee}(\bar{d}_R^{(1)} d_R^{(1)})$(keV)
600	14.58	6.73	9.74	3.64
800	19.31	8.79	12.97	4.82
1000	24.06	10.89	16.21	6.01
1200	28.82	13.00	19.45	7.20
1400	33.59	15.13	22.68	8.39
1600	38.36	17.25	25.92	9.59
1800	43.14	19.39	29.16	10.78
2000	47.92	21.52	32.40	11.98

where n is the principle quantum number. Putting these together, we find that

$$\Gamma_{ee} = \frac{e^4 \alpha_s^3(M_Q)}{27 n^3 \pi^2} M_V \left(1 - \frac{16\alpha_s}{3\pi}\right) \left(e_Q^2 + \frac{(g_V^Q)^2}{(1 - \kappa_Z)^2 \sin^4 2\theta_W}\right), \qquad (3.11)$$

where $\kappa_Z = m_Z^2 / M_V^2$. To get Eq. (3.11) we assumed that g_V^e is negligible and $\Gamma_Z^2 \kappa_Z \ll (1 - \kappa_Z)^2 M_V^2$, even though we have used the exact expressions for numerical calculations. In Table I, we have listed the decay width, Γ_{ee} for a range of KK-quarkonia masses.

We can now determine, using Eq. (3.5), the peak production cross sections for isodoublet and isosinglet KK-quarkonia. The results are show in Figs. 4 and 5. The cross sections are substantial, between 1 and 100 picobarns.

We now turn to the mass splittings between the different KK-quarkonia levels.

C. Mass Splittings

To observe KK-quark bound states, the mass splitting between adjacent resonances must be larger than their typical decay widths. The KK-quark mass scale justifies a non-relativistic calculation of the binding energies. We therefore solve the radial Schrödinger equation,

$$-\frac{1}{2\mu} \frac{d^2 u}{dr^2} + [V(r) + \frac{1}{2\mu} \frac{l(l+1)}{r^2}] u = \Delta E \, u, \qquad (3.12)$$
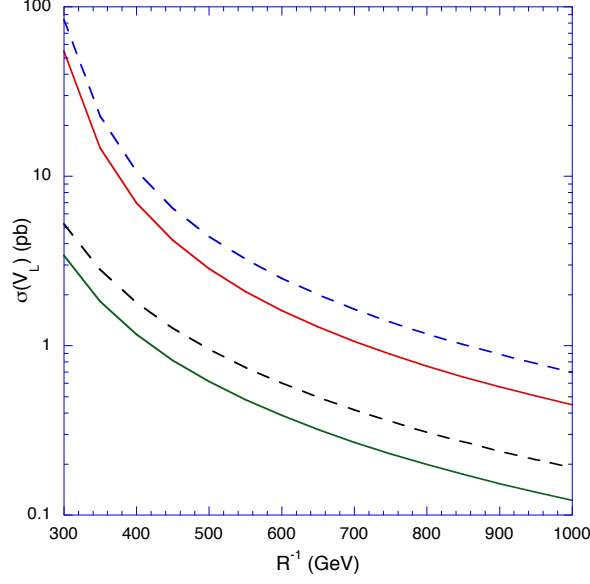
FIG. 4: The resonance production cross section for isodoublet KK-quarkonia states, except KK-toponium, as a function of R^{-1} for $\lambda R = 5$, 20. The solid lines represent down type KK-quarkonia states and the dashed ones represent up-type KK-quarkonia states, and the upper (lower) lines correspond to $\lambda R = 5\,(20)$.
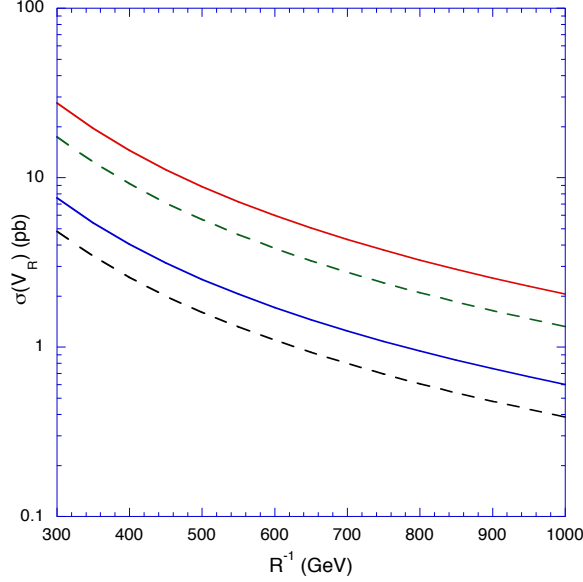

FIG. 5: The same as Fig. 4 but for isosinglet KK-quarkonia states. Here the upper (lower) lines correspond to $\lambda R = 20\,(5)$.

for a suitable phenomenological potential $V(r)$. Here $u(r) = rR(r)$ and the complete wave function is $\psi(r, \theta, \phi) = R(r)Y_{lm}(\theta, \phi)$. The wave function satisfies

$$u(0) = 0\,,$$

14

$$u(r) \rightarrow 0\,, \ r \rightarrow \infty\,. \tag{3.13}$$

Given a choice for $V(r)$, Eq.(3.12) is solved numerically to obtain the energy eigenvalues ΔE; the mass for each bound state is then given by

$$M_n = 2M_{KK} + \Delta E_n\,, \tag{3.14}$$

where ΔE_n is the energy eigenvalue of the nth level and M_{KK} is the mass of the KK-quark. Normalizing the wave function by

$$\int_0^\infty |u|^2 dr = 1\,, \tag{3.15}$$

one may compute $R(0) = u'(0)$.

QCD motivates the following form for the potential:

$$V = -\frac{4}{3}\frac{\alpha_s}{r} + Ar\,. \tag{3.16}$$

The first term is Coulomb-like and is generated by one-gluon exchange, while the second is linear and models confinement. For $A \simeq 1$ GeV fm^{-1}, this potential predicts energy level splittings in good agreement with the data for the Υ and J/ψ systems. At the typical energies of KK-quarkonia production, one would expect the Coulomb-like potential to dominate resulting in nearly hydrogen-like energy level splittings. However, hydrogen-like wave functions become more spread out at higher energy levels, suggesting a more significant contribution from the linear term in these cases. Note, however, that the level spacings for a hydrogen-like spectrum decrease roughly as $\Delta E_{n,n+1} \propto \dfrac{1}{n^3}$, where n is the radial quantum number. Therefore, only the first few energy levels will have splittings large enough to permit KK-quark bound states to be distinguished.

For $A = 1$ GeV fm^{-1} and $\alpha_s = 0.1$, the radial Schrödinger equation was solved numerically for the 1S, 2S, and 3S energy levels. The results are listed in Table II for KK-quark masses of 300 GeV and 500 GeV, along with the predictions of a hydrogen-like potential. As expected, both the energy eigenvalues and $R(0)$ are nearly hydrogen-like, justifying the use of Eq. (3.10) in the decay rate calculations.

We see that the mass splittings, especially between the 1S and 2S states, are substantially larger than the width of these states, and thus will be discernible in a collider with sufficient energy resolution. We now turn to experimental detection of these states.

TABLE II: Energy shifts and radial wave functions at the origin computed numerical assuming the potential in Eq. (3.16). The parameter a_0 here is $1/(\mu \alpha_s)$, where $\mu = M_{KK}/2$ is the reduced mass. The last two columns show the result obtained when neglecting the linear term in the potential.

M_{KK}	level	ΔE (GeV)	$a_0^{3/2} R(0)$	ΔE_H (GeV)	$a_0^{3/2} R(0)_H$
300	1S	-1.319	3.096	-1.334	3.079
300	2S	-0.276	1.173	-0.333	1.089
300	3S	-0.030	0.763	-0.149	0.593
500	1S	-2.213	3.085	-2.223	3.079
500	2S	-0.521	1.122	-0.555	1.089
500	3S	-0.171	0.670	-0.248	0.593

IV. DETECTION

The production cross section for KK-quarkonia at a linear collider can now be discussed. For definitiveness, we first consider the isosinglet KK-quarks, assuming $1/R = 500$ GeV and $\Lambda R = 20$. The masses of the $d_R^{(1)}$ and $s_R^{(1)}$ are then 572.14 GeV, the $b_R^{(1)}$ is 572.16 GeV, and the $u_R^{(1)}$ and $c_R^{(1)}$ are 573.84 GeV. (The mass of the $t_R^{(1)}$ is actually a few GeV lighter, but its decay signature, as noted in the last section, is completely different.)

Putting these together, we find the cross section as a function of $\sqrt{s}$ given in Fig. 6. The signature is very dramatic–one expects two monochromatic (in this case, 67 GeV) quarks and large missing energy. Clearly, the splitting between the resonances is large enough to separate the states. In the case of the top KK-quark, the resulting cross section looks identical to those of the up and charm KK-quark, but now the signature would be a fermion-antifermion pair, each with an energy of 570 GeV.

The masses of the isodoublet KK-quarks, except for the top, are nearly degenerate at 585.7 GeV. The cross section is plotted in Fig. 7. Again, the splitting between the resonances is large enough to separate the low-lying states. Here, the signatures are also dramatic, with two monochromatic quarks (in this case with energies of 46 GeV) and, depending on the decay chain, charged leptons, as discussed earlier. The isodoublet top KK-quark has a similar cross section, but is approximately 12 GeV heavier.
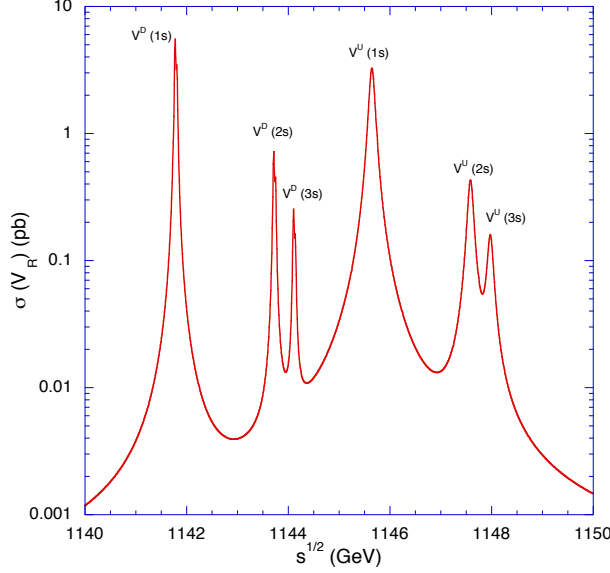
FIG. 6: The cross section for KK-quarkonia formed by isosinglet KK-quarks as a function of $\sqrt{s}$ for $1/R = 500$ GeV and $\Lambda R = 20$. The labels V^D refer to the bound states of isosinglet KK-down, KK-strange and KK-bottom quarks, while V^U refers to the bound states of isosinglet KK-up and KK-charm quarks.

These center-of-mass energies are rather high. However, the lower bound on the size of the extra dimensions is approximately 300 GeV. Using this value of $1/R$, we find the results in Figs 8 and 9, which are similar to the $1/R = 500$ GeV case. Note that one can discern the fact that the KK-bottom quark is slightly heavier than the KK-down and KK-strange quarks, leading to some substructure in the resonances. Of course, in all of these cases, the $n = 2$ modes will be out of reach of a TeV scale linear collider.

Of course, it will still not be possible to detect these structures if the beam resolution is too large. At a muon collider, this will not be a problem, since mass resolution of a few MeV is possible after deconvolution of the beamstrahlung and initial state radiation [10]. Resolution is a potential problem for electron-positron colliders, however, since one expects the average energy loss at $\sqrt{s} = 500$ GeV to be approximately 1.5% [11]. This energy loss comes from initial state radiation and beamstrahlung. However, the spectrum for each is well known and it is expected [11, 12] that the resulting mass resolution after deconvolution will be better than 10^{-4}, possibly a few times 10^{-5}, or 50 MeV for a $\sqrt{s} = 1000$ GeV. Such a mass resolution would easily allow the states to be detected (although precise width measurements would require better resolution). Clearly, a dedicated simulation would be
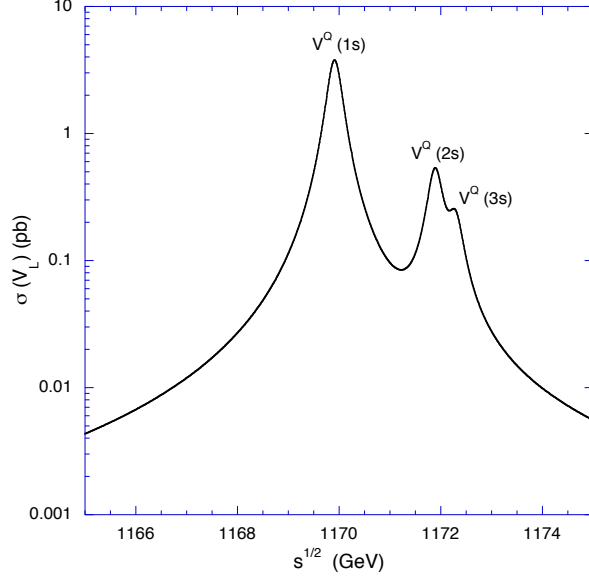
17

FIG. 7: The cross section for KK-quarkonia formed by isodoublet KK-quarks as a function of $\sqrt{s}$ for $1/R = 500$ GeV and $\Lambda R = 20$. The label V^Q refers to all of the isodoublet KK-quarks, except for the KK-top.
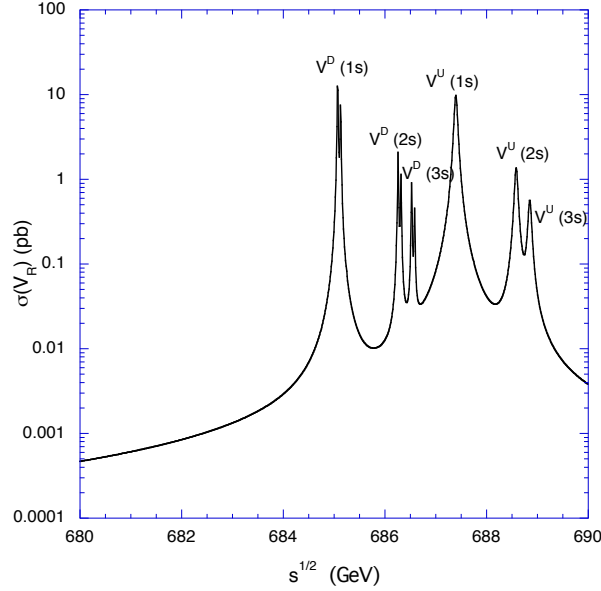

FIG. 8: The cross section for KK-quarkonia formed by isosinglet KK-quarks as a function of $\sqrt{s}$ for $1/R = 300$ GeV and $\Lambda R = 20$. The labels are the same as in the previous figures.

needed to determine the capabilities of a linear collider (such a simulation would also be relevant for long-lived fourth generation quarkonia, and other s-channel resonances) for detection of KK-quarkonia states.
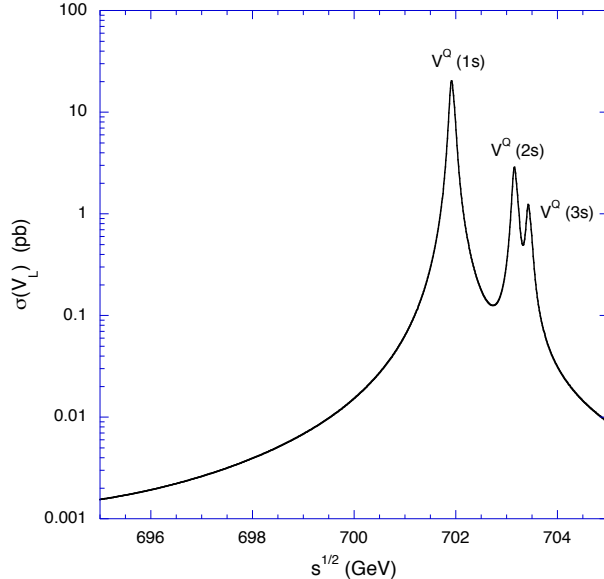
18

FIG. 9: The cross section for KK-quarkonia formed by isodoublet KK-quarks as a function of $\sqrt{s}$ for $1/R = 300$ GeV and $\Lambda R = 20$. The labels are the same as in the previous figures.

V.   CONCLUSIONS

If the simple model of Universal Extra Dimensions that we have considered is realized in nature, the mass splittings between the $n = 1$ KK-quarks and the lightest KK particle will be substantially smaller than the splitting between the top and bottom quarks. As a consequence, KK-quarks can be sufficiently long lived to form bound states, that we call KK-quarkonia, for a wide range of model parameters. With boundary mass corrections renormalized to vanish at an $\mathcal{O}(\text{TeV})$ cutoff scale Λ, we show that the KK-quark decay widths are in the 10-100 MeV range. We find that the peak cross sections for the 1S KK-quarkonia states are of the order of a few picobarns, and that the production cross sections near threshold show very clear and distinctive 1S, 2S and 3S resonant peaks. The decay signatures are very dramatic and nearly background-free: each isosinglet KK-quark (except the top) will decay into missing energy and a monochromatic quark (whose energy is determined solely by the KK-quark masses), and each isodoublet KK-quark will decay into missing energy, a monochromatic quark, and one or more leptons arising from subsequent two-body decays. The key issue for experimental detection is achieving sufficient energy resolution. This will not be a difficulty for a muon collider, and not impossible for an electron-positron machine. However, determining the resolution in the later case will require simulations to

19

deconvolve the beamstrahlung and initial state radiation energy loss mechanisms.

APPENDIX A: DECAY WIDTH FORMULAE

In this appendix, we give the partial decay width expressions for the decays of $n = 1$ KK-quarks by retaining all fermion masses and the mixing angle θ_1. For the decays of isosinglet KK-quarks, the partial decay widths can be expressed as

$$
\Gamma(d_R^{(1)} \to d_R\,\gamma^{(1)}) = \frac{e^2 m_{d_R^{(1)}} \cos^2\theta_1}{288\pi \cos^2\theta_W}\lambda^{1/2}(\kappa_\gamma,\kappa_d)\left[\frac{1}{\kappa_\gamma}\lambda(\kappa_\gamma,\kappa_d) + 3(-\kappa_\gamma + \kappa_d + 1)\right],
$$

$$
\Gamma(u_R^{(1)} \to u_R\,\gamma^{(1)}) = \frac{e^2 m_{u_R^{(1)}} \cos^2\theta_1}{72\pi \cos^2\theta_W}\lambda^{1/2}(\kappa_\gamma,\kappa_u)\left[\frac{1}{\kappa_\gamma}\lambda(\kappa_\gamma,\kappa_d) + 3(-\kappa_\gamma + \kappa_d + 1)\right],
$$

$$
\Gamma(d_R^{(1)} \to d_R\,Z^{(1)}) = \frac{e^2 m_{d_R^{(1)}} \sin^2\theta_1}{288\pi \cos^2\theta_W}\lambda^{1/2}(\kappa_Z,\kappa_d)\left[\frac{1}{\kappa_\gamma}\lambda(\kappa_\gamma,\kappa_d) + 3(-\kappa_\gamma + \kappa_d + 1)\right],
$$

$$
\Gamma(u_R^{(1)} \to u_R\,Z^{(1)}) = \frac{e^2 m_{u_R^{(1)}} \sin^2\theta_1}{72\pi \cos^2\theta_W}\lambda^{1/2}(\kappa_Z,\kappa_u)\left[\frac{1}{\kappa_\gamma}\lambda(\kappa_\gamma,\kappa_d) + 3(-\kappa_\gamma + \kappa_d + 1)\right], \quad \text{(A1)}
$$

and those for isodoublet case are

$$
\Gamma(d_L^{(1)} \to d_L\gamma^{(1)}) = \frac{e^2 m_{d_L^{(1)}}}{128\pi}\left[\frac{1}{3}\frac{\cos\theta_1}{\cos\theta_W} - \frac{\sin\theta_1}{\sin\theta_W}\right]^2\lambda^{1/2}(\kappa_\gamma,\kappa_d)\left[\frac{1}{\kappa_\gamma}\lambda(\kappa_\gamma,\kappa_d) + 3(-\kappa_\gamma + \kappa_d + 1)\right],
$$

$$
\Gamma(u_L^{(1)} \to u_L\gamma^{(1)}) = \frac{e^2 m_{u_L^{(1)}}}{128\pi}\left[\frac{1}{3}\frac{\cos\theta_1}{\cos\theta_W} + \frac{\sin\theta_1}{\sin\theta_W}\right]^2\lambda^{1/2}(\kappa_\gamma,\kappa_u)\left[\frac{1}{\kappa_\gamma}\lambda(\kappa_\gamma,\kappa_d) + 3(-\kappa_\gamma + \kappa_d + 1)\right],
$$

$$
\Gamma(d_L^{(1)} \to d_L Z^{(1)}) = \frac{e^2 m_{d_L^{(1)}}}{128\pi}\left[\frac{\cos\theta_1}{\sin\theta_W} + \frac{1}{3}\frac{\sin\theta_1}{\cos\theta_W}\right]^2\lambda^{1/2}(\kappa_Z,\kappa_d)\left[\frac{1}{\kappa_\gamma}\lambda(\kappa_\gamma,\kappa_d) + 3(-\kappa_\gamma + \kappa_d + 1)\right],
$$

$$
\Gamma(u_L^{(1)} \to u_L Z^{(1)}) = \frac{e^2 m_{u_L^{(1)}}}{128\pi}\left[\frac{\cos\theta_1}{\sin\theta_W} - \frac{1}{3}\frac{\sin\theta_1}{\cos\theta_W}\right]^2\lambda^{1/2}(\kappa_Z,\kappa_u)\left[\frac{1}{\kappa_\gamma}\lambda(\kappa_\gamma,\kappa_d) + 3(-\kappa_\gamma + \kappa_d + 1)\right],
$$

$$
\Gamma(u_L^{(1)} \to d_L W^{(1)}) = \frac{e^2 m_{u_L^{(1)}}}{64\pi \sin^2\theta_W}|V_{ij}|^2\lambda^{1/2}(\kappa_Z,\kappa_d)\left[\frac{1}{\kappa_\gamma}\lambda(\kappa_\gamma,\kappa_d) + 3(-\kappa_\gamma + \kappa_d + 1)\right], \quad \text{(A2)}
$$

where

$$
\lambda(x,y) = (1 - x - y)^2 - 4xy, \quad \kappa_q = \frac{M_q^2}{M_{KK}^2}, \quad \kappa_\gamma = \frac{M_{\gamma^{(1)}}^2}{M_{KK}^2}, \quad \kappa_Z = \frac{M_{Z^{(1)}}^2}{M_{KK}^2}, \quad \kappa_W = \frac{M_{W^{(1)}}^2}{M_{KK}^2}. \text{(A3)}
$$

and $q = u, d, s, c$ or b.

ACKNOWLEDGMENTS

———————————————

[1] I. Antoniadis, Phys. Lett. **B 246**, 377 (1990); J. D. Lykken, Phys. Rev. D **54**, 3693 (1996); N. Arkani-Hamed, S. Dimopoulos and G. Dvali, Phys. Lett. **B 429**, 263 (1998); I. Antoniadis, N. Arkani-Hamed, S. Dimopoulos and G. Dvali, Phys. Lett. **B 436**, 257 (1998).

[2] K. R. Dienes, E. Dudas and T. Gherghetta, Phys. Lett. **B 436** 55 (1998); Nucl. Phys. **B 548**, 47 (1999).

[3] P. Nath and M. Yamaguchi, Phys. Rev. D **60**, 116006 (1999); Phys. Rev. D **60**, 116004 (1999); M. Masip and A. Pomarol, Phys. Rev. D **60**, 096005 (1999); A. Strumia, Phys. Lett. B **466**, 107 (1999); R. Casalbuoni, S. De Curtis, D. Dominici and R. Gatto, Phys. Lett. B **462**, 48 (1999); C. D. Carone, Phys. Rev. D **61**, 015008 (2000); T. G. Rizzo and J. D. Wells, Phys. Rev. D **61**, 016007 (2000).

[4] T. Appelquist, H. -C. Cheng and B. A. Dobrescu, Phys. Rev. **D 64**, 035002 (2001).

[5] A. J. Buras, A. Poschenrieder, M. Spranger and A. Weiler, hep-ph/0306158 and references therein.

[6] H. -C. Cheng, J. L. Feng, K. T. Matchev, Phys. Rev. Lett. **89**, 211301 (2002); D. Majumdar, Mod. Phys. Lett. **A 18** 1705 (2003); D. Majumdar, Phys. Rev. **D 67**, 095010 (2003); G. Servant and T. M. P. Tait, Nucl. Phys. **B 650**, 391 (2003); D. Hooper and G. D. Kribs, Phys. Rev. **D 67**, 055003 (2003).

[7] H. -C. Cheng, K. T. Matchev and M. Schmaltz, Phys. Rev. **D 66**, 036005 (2002).

[8] H. -C. Cheng, K. T. Matchev and M. Schmaltz, Phys. Rev. **D 66**, 056006 (2002).

[9] V. D. Barger and R. J. N. Phillips, *Collider Physics*, Frontiers in Physics, Vol. 71, Addision-Wesley, 1996.

[10] G. G. Hanson, Nucl. Instrum. Meth. A **503**, 96 (2003); C. M. Ankenbrandt et al., Phys. Rev. ST Accel. Beams 2, 081001 (1999).

[11] See K. Monig, LC-PHSM-2000-60-TESLA, available at http://www-flc.desy.de/lcnotes/, and references therein.

[12] See G. Wilson, LC-PHSM-2001-009-TESLA, available at http://www-flc.desy.de/lcnotes/, and references therein. We thank Ayres Freitas for these references and a discussion.